ELSEVIER

Biochemical Pharmacology 63 (2002) 1099–1111

Biochemical Pharmacology

BGP-15 — a novel poly(ADP-ribose) polymerase inhibitor — protects against nephrotoxicity of cisplatin without compromising its antitumor activity

Ildiko Racz[a], Kalman Tory[a], Ferenc Gallyas Jr.[b], Zoltán Berente[b], Erzsebet Osz[c], Laszlo Jaszlits[a], Sandor Bernath[a], Balazs Sumegi[b], Gyorgy Rabloczky[a], Peter Literati-Nagy[a,*]

[a]*N-Gene R&D, Szent Istvan Krt. 18, Budapest, Hungary*
[b]*Department of Biochemistry, Faculty of Medicine, University of Pecs, Pecs, Hungary*
[c]*Department of Medical Chemistry, Faculty of Medicine, University of Pecs, Pecs, Hungary*

Received 7 September 2001; accepted 4 December 2001

Abstract

Nephrotoxicity is one of the major dose limiting side effects of cisplatin chemotherapy. The antitumor and toxic effects are mediated in part by different mechanisms, thus, permitting a selective inhibition of certain side effects. The influence of *O*-(3-piperidino-2-hydroxy-1-propyl)nicotinic amidoxime (BGP-15) — a poly(ADP-ribose) polymerase (PARP) inhibitor — on the nephrotoxicity and antitumor efficacy of cisplatin has been evaluated in experimental models. BGP-15 either blocked or significantly reduced (60–90% in 100–200 mg/kg oral dose) cisplatin induced increase in serum urea and creatinine level in mice and rats and prevented the structural degeneration of the kidney, as well. The nephroprotective effect of BGP-15 treatment was revealed also in living mice by MRI analysis manifesting in the lack of oedema which otherwise developed as a result of cisplatin treatment. The protective effect was accompanied by inhibition of cisplatin-induced poly-ADP-ribosylation and by the restoration of the disturbed energy metabolism. The preservation of ATP level in the kidney was demonstrated *in vivo* by localized NMR spectroscopy. BGP-15 decreased cisplatin-induced ROS production in rat kidney mitochondria and improved the antioxidant status of the kidney in mice with cisplatin-induced nephropathy. In rat kidney, cisplatin caused a decrease in the level of Bcl-x, a mitochondrial protective protein, and this was normalized by BGP-15 treatment. On the other hand, BGP-15 did not inhibit the antitumor efficacy of cisplatin in cell culture and in transplantable solid tumors of mice. Treatment with BGP-15 increased the mean survival time of cisplatin-treated P-388 leukemia bearing mice from 13 to 19 days. PARP inhibitors have been demonstrated to diminish the consequences of free radical-induced damage, and this is related to the chemoprotective effect of BGP-15, a novel PARP inhibitor. Based on these results, we propose that BGP-15 represents a novel, non-thiol chemoprotective agent.

Keywords: Chemoprotection; Cisplatin; Side effect; Poly(ADP-ribose) polymerase; Nephrotoxicity

1. Introduction

Cisplatin is one of the most frequently used anticancer agents. It is highly effective against ovarian, testicular, bladder, head and neck, osteogenic and uterine cervics carcinomas. Unfortunately, high-dose cisplatin therapy is often accompanied by serious side effects affecting the kidney, peripheral neurons, and cochlea, which may force termination of the treatment or dose reduction.

Cisplatin-induced renal toxicity is characterized by reduced renal blood flow and proximal tubule injury. Intensive hydration in combination with forced diuresis, addition of hypertonic saline, and the use of chemoprotective agents provide some protection against cisplatin-induced nephrotoxicity [1]. Most of the chemoprotective agents in clinical use for reducing side effects of cisplatin, such as amifostine, diethylthiocarbamates, sodium thiosulfate and glutathione possess thiol group. Of these drugs, amifostine has gained the most widespread clinical application. Amifostine is a prodrug, which is converted by membrane bound alkaline phosphatases to a free sulfhydryl containing compound, and this binds directly to active derivatives of cisplatin [2]. However, neither amifostine nor other treatments provide complete protection against the nephrotoxic effect of cisplatin, especially against long-term damages.

* Corresponding author.
E-mail address: ngene@mail.datanet.hu (P. Literati-Nagy).

0006-2952/02/$ – see front matter
PII: S0006-2952(01)00935-2

The exact mechanism of cisplatin-induced nephrotoxicity is not yet clear. Cisplatin generates reactive oxygen species (ROS), superoxide anions and hydroxyl radicals [3,4], which in turn cause oxidative damage in the kidney [5,6]. The protective effect of free radical scavengers and antioxidants in cisplatin-induced nephrotoxicity supports the central role of oxidative damage in the pathomechanism of the disease [7]. Mitochondria, where endogenous free radicals are mostly generated are also affected by cisplatin. It has been proposed that mitochondrial dysfunction and an increased release of free radicals may directly contribute to cytotoxicity during cisplatin chemotherapy [8]. Reactive oxygen species induce single-strand DNA breaks, which, in turn, activate nuclear PARP (E.C. 2.4.2.30). Indeed, activation of PARP has been observed in cisplatin-treated cells [9]. Excessive PARP activation depletes its substrate, NAD^+ and subsequently ATP, which eventually leads to cell death. PARP inhibitors can prevent overactivation of the enzyme and the subsequent energy crisis thereby saving the cell. Indeed, beneficial effects of PARP inhibition have been documented in various diseases where oxidative damage plays an important role in the pathomechanism.

BGP-15, is a nicotinic amidoxime derivative with PARP inhibitory activity. It has been demonstrated that BGP-15 protects against ischemia-reperfusion injury [10]. In the present paper, we investigated the effect of BGP-15 on the nephrotoxicity and antitumor activity of cisplatin in rat and mouse experimental models.

2. Materials and methods

2.1. Animals

NMRI CV1 mice for the nephrotoxicity studies, BD2F1 mice for the tumor studies, and Wistar rats were purchased from Charles River Hungary Breeding Ltd. The animals were kept under standardized conditions; tap water and rat chow were provided *ad libitum*. Animals were treated in compliance with approved institutional animal care guidelines.

2.2. Chemicals

Cisplatin-TEVA and Amifostine were obtained from TEVA Pharma and Schering-Plough Ltd., respectively. Thiopental sodium and diazepam were purchased from Byk Gulden (Germany) and Richter (Hungary). All other chemicals were purchased from Sigma. Cell culture tools were Falcon and Corning products. BGP-15 was synthesized in the Institute for Drug Research Ltd., Hungary.

2.3. Cisplatin-induced nephrotoxicity model

Nephrotoxicity was induced in mice and rats by single and repeated administration of cisplatin. Mice received 20 mg/kg (i.p.) cisplatin in single dose experiments, and 3.8 mg/kg per day or 5 mg/kg per day cisplatin for 5 consecutive days i.p. in the repeated dose experiments. In rats, repeated doses of cisplatin (5×2 and 5×2.5 mg/kg doses) were used to induce nephropathy.

Dosing schedules in experiments were as follows:

1. Groups of six mice were treated with a single 20 mg/kg, i.p. dose of cisplatin with and without BGP-15 (100 mg/kg, p.o.). Animals were sacrificed on day 4.
2. Groups of 10 mice were treated with two doses of cisplatin (3.8 and 5 mg/kg, i.p.) with and without BGP-15 (200 mg/kg, p.o.) for 5 consecutive days. BGP-15 treatment continued for 2 additional days. Animals were sacrificed on day 7.
3. Groups of 10 rats were treated with cisplatin (2 mg/kg, i.p.) with and without BGP-15 (100, 200 mg/kg, p.o.) for 5 consecutive days. BGP-15 treatment continued for 2 additional days. Animals were sacrificed on day 11.
4. B-16 tumor bearing mice were treated as in the second experiment.

Renal damage was assessed by monitoring blood urea and serum creatinine levels, and by histological and MRI analysis. Urea and creatinine levels were determined by UV photometry [11,12] and by Jaffe's kinetic method [13,14], respectively. Formalin-fixed, paraffin-embedded kidney sections were stained with hematoxylin–eosin. Tissue sections were evaluated under a light microscope, and damage scores were determined by an examiner who was blind to the experiment. Tubular degeneration was classified by their extent as focal (effecting only a part of the tubulus) or diffuse (effecting several tubuli) and by their severity as (1) mild, (2) moderate, (3) severe (including focal necrosis). The differences between total scores of the groups were examined with Kruskal–Wallis ANOVA test.

BGP-15 was dissolved in water or physiological saline and administered 15–30 min prior to cisplatin treatment. Amifostine was used as a reference chemoprotective agent, and was administered i.p. according to the same schedule as BGP-15.

2.3.1. MRI analysis

Groups of five mice were treated with 5 mg/kg cisplatin (i.p.) for 5 consecutive days with and without BGP-15 (100 mg/kg, p.o.). The mice were sedated on day 7 with a mixture of thiopental sodium (25 mg/kg) and diazepam (5 mg/kg) administered i.p. and were placed into an epoxy resin animal holder tube.

MRI measurements were performed on a Varian ^{UNITY}INOVA 400 spectrometer (Varian, Inc.) with a 89 mm vertical bore magnet of 9.4 T (Oxford Instruments Ltd.) using a 35 mm inner diameter hollow microimaging probe with built-in self-shielded gradient system up to 400 mT/m (Doty Scientific, Inc.). After tuning, shimming (^{1}H linewidth of $\approx$150 Hz) and RF calibration, the location

of the kidneys was determined using a multislice spin-echo sequence (TR = 1000 ms, TE = 12 ms). T_2-weighted images were recorded using multislice spin-echo sequence (4.0 ms sinc pulses, TR = 3000 ms, TE = 50 ms, slice thickness = 1 mm, FOV = 30 mm × 30 mm, acquisition matrix 128 × 128). One average was taken and images were reconstructed as 256 × 256 matrices.

2.4. Evaluation of the poly(ADP-ribose) content and energy metabolism in the kidney

2.4.1. Western blot analysis of poly-ADP-ribosylation

Group of four C57Bl mice were treated on 5 consecutive days with cisplatin (3.8 mg/kg, i.p.), cisplatin (same dose) in combination with BGP-15 (100 mg/kg, p.o.) or vehicle. On the following day animals were sacrificed and kidneys were excised and homogenized in cold buffer containing 10 mM Tris–HCl, pH 8.0, 2 mM DTT, 0.1 mM PMSF, 10 μg/mL leupeptin and 0.25 mM sucrose then samples were centrifuged for 5 min at 14,000 *g* and the pellet was resuspended in the same buffer. Protein concentration was determined with Bradford assay and 40 μg of protein were loaded on SDS-PAGE gel. Protein was transferred to Hybond-P membrane (Amersham) and was incubated with 1:2000 dilution of anti-poly(ADP-ribose) polyclonal antibody (LP96-10, Biomol). Specifically bound antibody was visualized with peroxidase-conjugated anti-rabbit antibody and with enhanced chemiluminescence reagent (Amersham). Films were scanned and integrated density was evaluated by the ImageTool program Version 2 (University of Texas).

2.4.2. Analysis of energy metabolism by localized ^{31}P NMR spectroscopy

Measurements were performed on a Varian ^{UNITY}INOVA 400 spectrometer with a 89 mm vertical bore magnet of 9.4 T field strength using a 35 mm inner diameter hollow multinuclear microimaging probe with Litz volume coil for ^1H studies, R1T volume coil for ^{31}P studies and built-in self-shielded gradient system up to 400 mT/m (Doty Scientific, Inc.).

Mice were divided into three groups. The first (control) group was injected with saline intraperitoneally. The second group was injected with 3.8 mg/kg per day cisplatin intraperitoneally. The third group was injected i.p. with 3.8 mg/kg per day cisplatin and 100 mg/kg per day BGP-15 orally. After 5 days treatment, mice underwent localized NMR spectroscopic experiments. Before spectroscopy, mice were anaesthetized by urethane.

In vivo localized ^{31}P NMR spectra were recorded by employing the ISIS pulse sequence (repetition time = 4000 ms, middle interval = 1 ms, adiabatic Gaussian inversion pulses and 90° square readout pulses) after planning the voxels of interest using spin-echo scout images (repetition time = 1000 ms, echo time = 12 ms) recorded in transversal and coronal orientations. Voxels (typically 6 mm × 4 mm × 2 mm) were planned to contain kidney tissue only (see Fig. 7a). For all kidneys, phosphorus metabolite levels were quantified after deconvolution of the spectra using Vnmr 6.1B software (Varian Inc.) provided with the spectrometer. In order to maintain non-invasive conditions, no internal standard was used; therefore, sample-to-sample comparisons of the metabolite levels would not be reliable enough. Thus, ratios of the metabolites (ATP/ADP ratio, ATP/P_i ratio and phosphorylation potential [ATP/(ADP·P_i)]) were calculated for each kidney. Data were expressed as mean ± SEM, statistical analysis was performed by ANOVA.

2.5. Evaluation of the antioxidant status in nephropathy

2.5.1. Determination of renal glutathione content

Groups of five CD-1 mice were treated with 5 mg/kg cisplatin i.p. for 5 consecutive days either by itself or in combination with 100 mg/kg BGP-15. BGP-15 was administered orally. On day 7, the kidneys were perfused with cold physiological saline and renal GSH content was determined according to Beutler *et al.* [15].

2.5.2. Determination of renal superoxide dismutase and catalase activity

Groups of six CD-1 mice were treated as above, but BGP-15 was applied in 200 mg/kg dose. Renal catalase activity was measured by the method of Aebi [16]. Briefly, tissue extract was prepared in phosphate-EDTA buffer. Ethanol (20 μL) was added to 200 μL extract and the mixture was kept on ice for 30 min, then 20 μL Triton X-100 was added. In all, 250 μL of treated extract was added to equal volume of 0.066 M H_2O_2 and change of the optical density was measured at 240 nm for 30 s. The molar extinction of 43.6 M/cm was used to calculate catalase activity.

SOD activity was determined according to the method of Misra and Fridovich [17]. Tissue extract was added to 880 μL sodium carbonate (0.05 M, pH 10.2; 10^{-4} M EDTA) buffer. Then 20 μL of 30 mM epinephrine (dissolved in 0.5% acetic acid) was added to the reaction mixture. The production of adrenochrom was measured at 480 nm for 4 min at 30°. SOD activity is expressed as the amount of enzyme that inhibits the autooxidation of epinephrine by 50%.

2.5.3. Protein assay

Protein concentration of kidney homogenates was determined by Bradford reagent (Sigma) according to the manufacturer's recommendation, using serum albumin as standard.

2.6. Evaluation of the Bcl-x(L) content of the kidney

Kidney samples were homogenized in 20 mM Tris–HCl buffer, pH 7.4 containing 3 mM EDTA, 5 mM mercap-

toethanol and 1% SDS with Ultra Turrax homogenizer. After the addition of 1% bromphenol blue, samples were boiled for 2 min and clarified by centrifuging (8000 *g* for 2 min). Sodium dodecylsulfate-polyacrylamide gel electrophoresis was carried out on 12% gel. A low molecular weight calibration kit (Pharmacia) was used for estimation of the molecular weight. For immunoblotting, separated proteins were transferred to nitro-cellulose filters. The filters were blocked with 2% no-fat milk in TBS (150 mM NaCl, 20 mM Tris–HCl, pH 7.5) containing 1% polyethylene glycol 6000, and incubated with anti-Bcl-x(L) (monoclonal antibody) or anti-lactate dehydrogenase polyclonal antibodies diluted in the same solution. Adsorbed IgG was detected by either anti-mouse IgG peroxidase complex or anti-rabbit IgG peroxidase complex and visualized by enhanced chemiluminescence (ECL) method. Western blot data were analyzed by ImageTool image processing program.

2.7. Evaluation of the ROS production in rat mitochondria

ROS formation was detected using the oxidation-sensitive non-fluorescent probe dihydrorhodamine123, which can be oxidized by ROS to fluorescent rhodamine123 [18]. Cisplatin and cisplatin + BGP-15 (100 mg/L) were added to isolated rat kidney mitochondria in the presence of 1 μM dihydrorhodamine123 and the formed rhodamine123 was monitored by a Perkin-Elmer fluorescence spectroscope at an excitation wavelength of 496 nm and an emission wavelength of 536 nm.

2.8. Antitumor assays

2.8.1. In vitro cytotoxicity assay

Human tumor cell lines A549, HCT-15, HCT-116, and Du-145 were maintained in RPMI 1640 medium supplemented with 10% FCS in humidified air containing 5% CO_2. For *in vitro* cytotoxicity assays, 5×10^3 to 5×10^4 cells were plated into the wells of 96-well plates in 100 μL culture medium. On the following day, cells were exposed to BGP-15 (10, 30, 100 μg/mL) and to a series of concentrations of cisplatin either by itself or in combination. Cultures were incubated in a total volume of 200 μL for 3 more days at 37°. Samples were prepared in duplicates or triplicates. Cell growth was evaluated by MTT or SRB assays [19]. Growth inhibition curves were calculated.

2.8.2. Transplantable mouse tumors

Transplantable mouse tumors S-180 sarcoma, B-16 melanoma, and P-388 leukemia were obtained from the National Cancer Institute (Frederick) and tumors were maintained by serial subcutaneous and intraperitoneal transplantation. B-16 and S-180 tumors were transplanted by tissue homogenate containing 50 mg tumor tissue or 10^6 tumor cells. Treatment of animals started when the transplanted tumors reached 3–5 mm in diameter. Tumor sizes were either measured percutaneously with a caliper and tumor volumes were calculated from the perpendicular diameters or tumors were excised at the termination of the experiment and tumor weights were measured.

P-388 leukemia was transplanted by 5×10^6 cell i.p. Cisplatin treatments (10 mg/kg, i.p.) were applied on days 3 and 10. BGP-15 was administered in 100 mg/kg daily oral doses from the third day throughout of the experiment. Survival time was recorded till the 35th day of the experiment.

3. Results

3.1. Effect on nephrotoxicity

The applied single and repeated dose cisplatin treatment resulted in reproducible renal damage both in mice and rats as evidenced by increased blood urea (25–50 mmol/L) and serum creatinine (100–300 μmol/L) levels. In mice, administration of BGP-15 in 100 mg/kg oral dose prevented the single dose (20 mg/kg, i.p.) cisplatin induced increase in urea and creatinine levels on day 4 (Fig. 1). Similarly to single application, administration of BGP-15

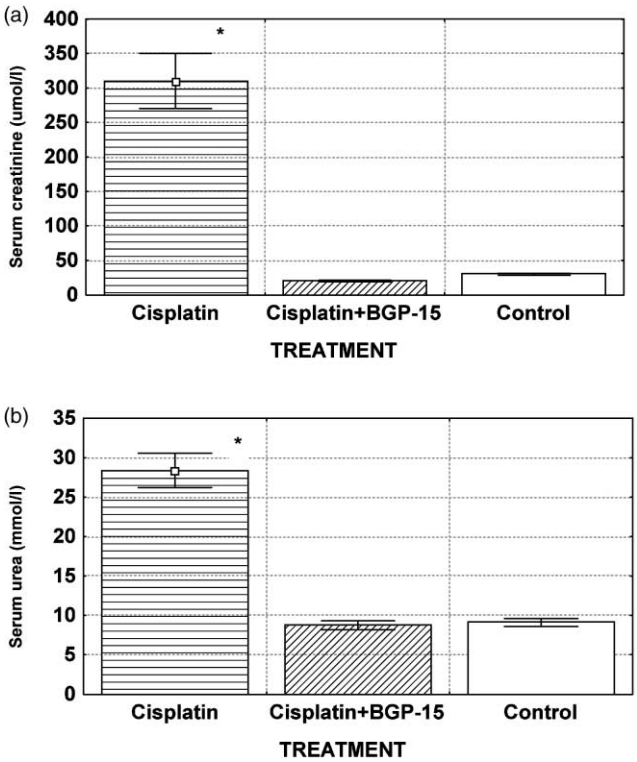

Fig. 1. Effect of cisplatin (20 mg/kg, i.p.) and cisplatin + BGP-15 (100 mg/kg, p.o.) on serum creatinine (a) and blood urea (b) concentration in mice 4 days after treatment. Mean values ± SEM are shown. The asterisk (*) values are different ($P < 0.05$) as compared to BGP-15-treated and control groups.

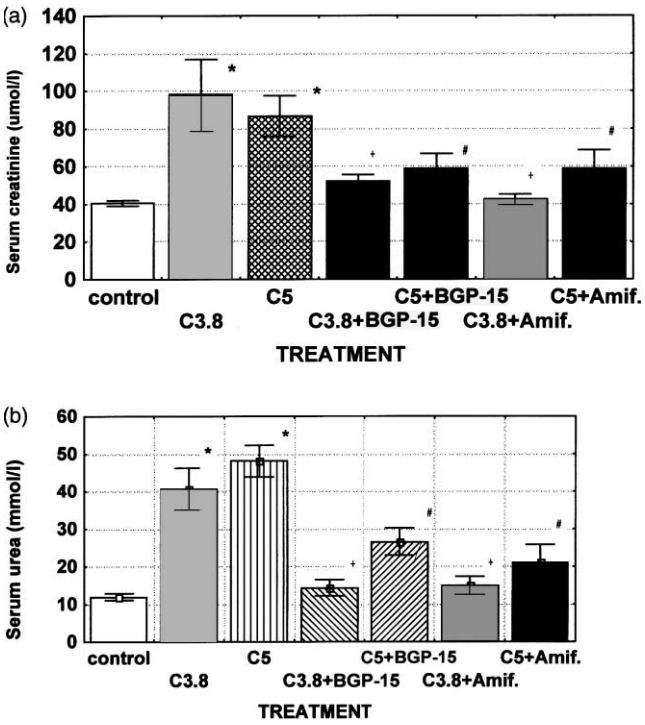

Fig. 2. Serum creatinine (a) and urea (b) concentrations in cisplatin-induced acute renal failure. Mice were treated for 5 consecutive days with cisplatin (3.8/C3.8 and 5.0/C5/mg/kg, i.p.), cisplatin + BGP-15 (200 mg/kg, p.o./C3.8 + BGP and C5 + BGP) and cisplatin + amifostine (200 mg/kg, i.p./C3.8 + amifostine and C5 + amifostine). The concentration of serum creatinine and urea was evaluated on day 7. Mean values ± SEM are shown. Values are different ($P < 0.05$) as compared to control (∗), 3.8 mg/kg cisplatin (+), and 5 mg/kg cisplatin (#).

in 200 mg/kg oral dose almost completely blocked the increase in urea and creatinine levels when it was induced by repeated doses of cisplatin (5 × 3.8 mg/kg). When cisplatin was used at higher doses (5 × 5 mg/kg), BGP-15 inhibited the effects of cisplatin by more than 50% (Fig. 2). Intraperitoneally administered amifostine (200 mg/kg) had a similar protection against cisplatin-induced nephrotoxicity (Fig. 2). The nephroprotective effect of BGP-15 treatment was somewhat less pronounced in rat than in mice, but it still resulted in a substantial and significant protection as suggested by changes in blood urea and serum creatinine levels (Fig. 3).

Histological examination revealed focal tubular degeneration in mice after low dose (3.8 mg/kg) cisplatin treatment. Treatment with higher (5 mg/kg) cisplatin dose morphological signs of extensive tubular degeneration were manifested, which were largely prevented by BGP-15 (Fig. 4). The score values of histological alterations are listed in Table 1. This valuation also demonstrates that BGP-15 significantly alleviates morphological alterations (Kruskal–Wallis, $P = 0.02$).

MRI analysis of mice kidney have demonstrated that T_1-weighted transverse spin-echo images (TR = 1000 ms, TE = 12 ms, 118 μm × 118 μm × 1 mm resolution) were rather indistinguishable. In contrast, T_2-weighted transverse spin-echo images (TR = 3000 ms, TE = 50 ms, same resolution) showed marked differences in the peripheral regions of the kidneys (Fig. 5). In control animals, the kidney tissues appeared to be rather homogeneous, whereas animals treated with cisplatin showed marked increase of intensity in the peripheral regions, probably due to an increase in the "free" water content (oedema) of the tissues. In animals treated with cisplatin and BGP-15, the increase in intensity was considerably smaller.

Cisplatin treatment resulted in serious general toxicity and lethality. The primary cause of lethality in mice was gastrointestinal damage rather than renal failure. Daily administration of 200 mg/kg BGP-15 during 5 × 3.8 mg/kg, i.p. cisplatin treatment increased the survival rate from 5/15 to 9/15 ($P = 0.06$).

3.1.1. Effect on the poly(ADP-ribose) content

The applied cisplatin treatment significantly increased the poly(ADP-ribose) content of the kidney (Fig. 6). The means ± SEM of integrated densities in arbitrary units

Table 1
Individual and total score values of tubular degeneration in the kidney section of mice

Control		Treatment			
		Cisplatin 5 × 5 mg/kg, i.p.		Cisplatin 5 × 5 mg/kg, i.p. + BGP-15 5 × 100 mg/kg, p.o.	
Focal	Diffuse	Focal	Diffuse	Focal	Diffuse
0	0	0	3	0	0
0	0	1	0	0	0
0	0	0	1	0	0
0	0	0	2	0	0
1	0	0	3	1	0
			Total score		
1	0	1	9	1	0

Mice were treated for 5 consecutive days with 5 mg/kg cisplatin intraperitoneally with and without the addition of BGP-15 in 100 mg/kg daily oral dose. Kidneys were removed on day 7. Focal and diffuse tubular degenerations were scored separately as follows: (0) no specified change, (1) mild change, (2) moderate change, (3) severe change. The difference between the total scores of the cisplatin- and cisplatin + BGP-15-treated groups is significant ($P = 0.02$, Kruskal–Wallis ANOVA).

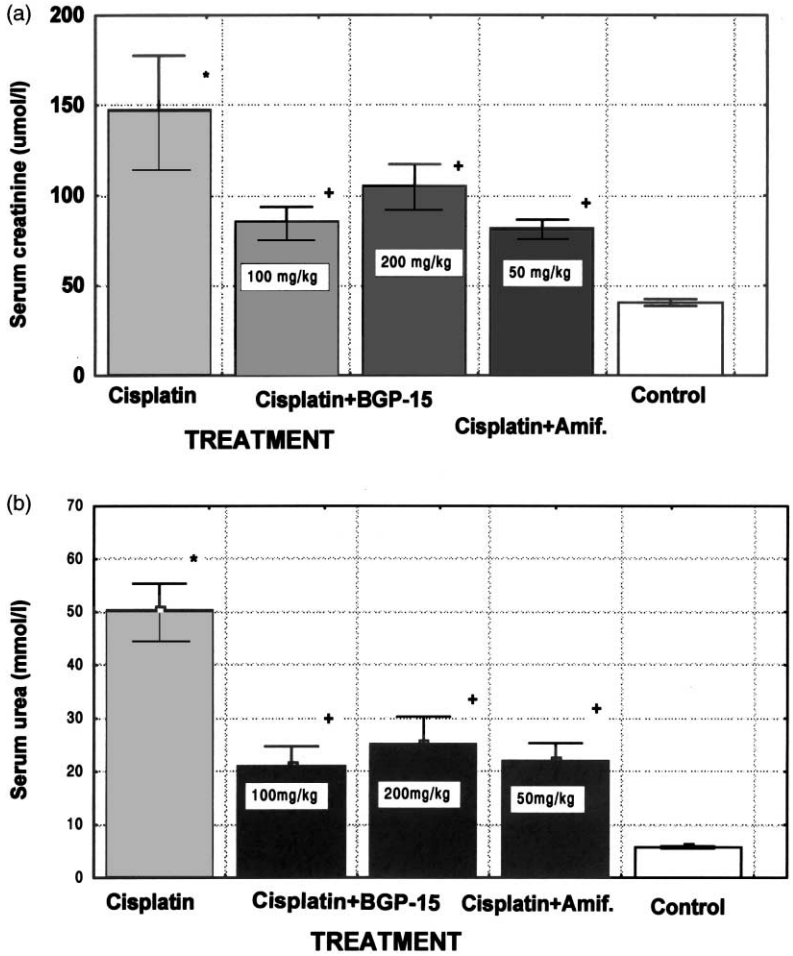

Fig. 3. Serum creatinine (a) and urea levels (b) in cisplatin-induced nephrotoxicity. Rats were treated for 5 consecutive days with cisplatin (5 × 2 mg/kg, i.p.), cisplatin + BGP-15 (100, 200 mg/kg, p.o.) or cisplatin + amifostine (50 mg/kg, p.o.). Serum creatinine levels were evaluated on day 10. Mean values ± SEM are shown. Values are different ($P < 0.05$) as compared to control (∗), 2 mg/kg cisplatin treatment (+).

were the following: cisplatin, 80.1 ± 8.1; cisplatin + BGP-15, 50.3 ± 10.2; control, 46.6 ± 11.3. BGP-15 treatment normalized the elevated poly-ADP-ribosylation.

3.1.2. *In vivo* determination of phosphorus metabolite levels by localized ^{31}P NMR spectroscopy

Selection of the area for localized ^{31}P NMR spectroscopy is demonstrated in Fig. 7a. Representative spectra are shown in Fig. 7b indicating that cisplatin causes a decrease in ATP level. BGP-15 treatment combined with cisplatin prevents the ATP decreasing effect of cisplatin. Quantitative data analysis is presented in Table 2. Data show that cisplatin induced decrease in ATP/ADP ratio, ATP/P_i ratio and phosphorylation potential. These changes were reverted by BGP-15 treatment.

3.1.3. *Influence on the antioxidant status of the kidney*

Glutathione level was by 31% ($P < 0.05$) higher in animals treated with cisplatin + BGP-15 as compared to that in cisplatin-treated groups. The same cisplatin treatment had no significant influence on SOD activity, while catalase activity was 30% higher ($P < 0.05$) in cisplatin + BGP-15-treated group than in the cisplatin-treated group (data not shown).

Table 2
Quantitative determination of ATP/ADP ratio, ATP/P_i ratio and phosphorylation potential in mice kidneys *in vivo*

Metabolite ratio	Control	Cisplatin	Cisplatin + BGP-15
ATP/ADP	2.75 ± 0.21	1.91 ± 0.20	2.72 ± 0.18
ATP/P_i	1.63 ± 0.06	1.20 ± 0.05	1.61 ± 0.06
ATP/(ADP·P_i)	(1.13 ± 0.09) × 10^{-3}	(0.61 ± 0.08) × 10^{-3}	(1.10 ± 0.07) × 10^{-3}

Animal treatments and *in vivo* determination of metabolite levels by localized ^{31}P NMR spectroscopy is described in Section 2. Values are mean ± SEM for five animals. Significant difference could be observed for control vs. cisplatin-treated ($P < 0.05$) and cisplatin-treated vs. cisplatin + BGP-15-treated animals ($P < 0.05$).

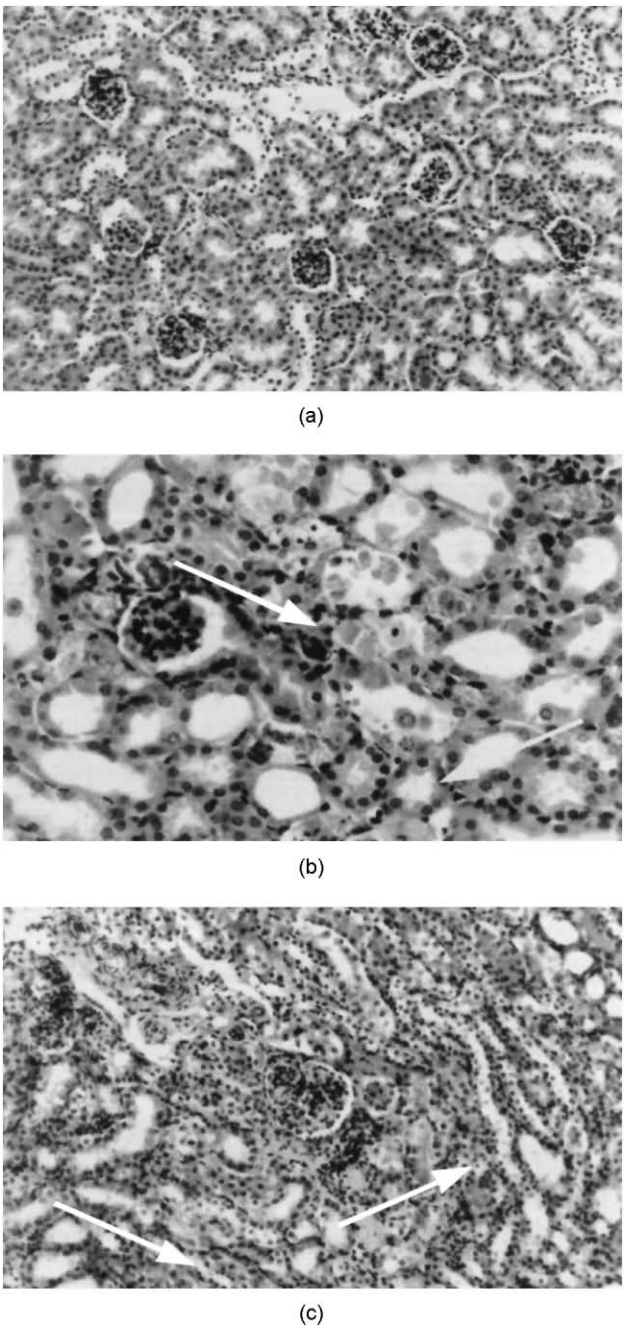

Fig. 4. Histology of the kidney. Mice were treated with 5 mg/kg cisplatin i.p. for 5 days either with or without the addition of BGP-15 (100 mg/kg per day, p.o.). Kidneys were removed on day 7. Sections were stained with hematoxilin–eosin. The tissue of normal kidney is shown in (a). Cisplatin treatment (b) results in oedomatous tissue, atrophic epithelium of tubuli and tubular degeneration (arrows). BGP-15 largely prevents the effects of cisplatin (c). Original magnification 300×.

3.1.4. Effect on the Bcl-x content of kidney

Western blot analysis of kidneys of cisplatin-treated animals showed a significant (about 80%) decrease in Bcl-x quantity as compared to that in control tissue, which may contribute to the defective function of mitochondria following cisplatin treatment. Combined treatment of animals with cisplatin and BGP-15 abrogated the cisplatin-induced decrease in Bcl-x content (Fig. 8).

Table 3
Effect of cisplatin on the mitochondrial ROS production in rat kidney mitochondria

Cisplatin (μM)	Rhodamine123 fluorescence in arbitrary units	
	0[a]	100[a]
0	0.4 ± 0.3	0.3 ± 0.2
37.5	9.0 ± 0.5	7.5 ± 0.4*
75	11.7 ± 0.4	10.7 ± 0.3
150	14.1 ± 0.4	11.4 ± 0.5*
300	15.2 ± 0.5	13.4 ± 0.4*

Values are means ± SEM for five experiments.
[a] Concentration of BGP-15 in mg/L.
* Values are different ($P < 0.05$) between BGP-15 treated and untreated samples.

3.1.5. Effect on mitochondrial ROS production

Mitochondrial ROS production was detected by determining the oxidation of non-fluorescent dihydrorhodamine123 to fluorescent rhodamine123. It was found that cisplatin treatment increased the mitochondrial ROS formation in a dose-dependent manner, and this was moderately decreased by BGP-15 (Table 3).

3.1.6. Effect on antitumor activity

BGP-15 did not have significant effects on the dose–growth inhibition curve of cisplatin *in vitro* in A549, HCT-15, HCT-116, and Du-145 human tumor cell lines (data not shown). The influence of BGP-15 on the antitumor activity of cisplatin *in vivo* was evaluated in three transplantable mouse tumors. Cisplatin and cisplatin + BGP-15 treatments resulted in 87 and 95% growth inhibition of the S-180 sarcoma 16 days after tumor transplantation. Tumor growth curves are shown in Fig. 9a. In B-16 melanoma bearing mice, cisplatin treatments (5 × 3.8 and 5 × 5 mg/kg, i.p.) inhibited tumor growth by 69 and 80%, respectively (Fig. 9b). Combined treatment with BGP-15 resulted in 79 and 81% growth inhibition (Fig. 9b). The nephrotoxic side effect of cisplatin was fully inhibited by BGP-15 in tumorous animals (data not shown) as well. In P-388 mouse leukemia combined treatment significantly increased the average survival time and the rate of long-term survival (Fig. 10) (Wilcoxon test, $P = 0.027$).

4. Discussion

The effect of BGP-15 was evaluated on cisplatin-induced nephrotoxicity and antitumor activity. BGP-15 administered in 100–200 mg/kg oral doses shortly before cisplatin treatment either prevented or significantly inhibited the development of cisplatin-induced acute renal failure as evidenced by functional and morphological findings. The nephroprotective effect was accompanied by the normalization of the cisplatin induced increase in poly-ADP-ribosylation and by the preservation of ATP level in the kidney. BGP-15 had a significant effect on the antioxidant

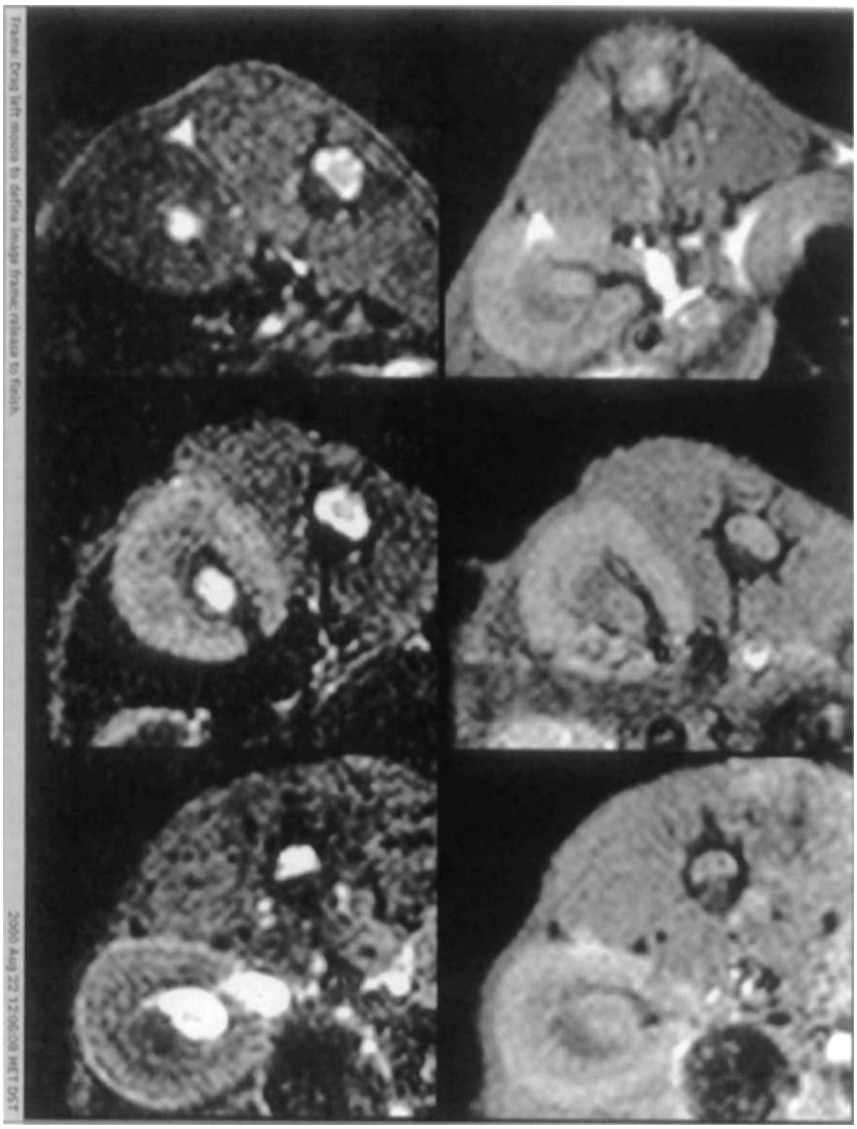

Fig. 5. Effect of cisplatin treatment on T_1- and T_2-weighted image of mice kidney. T_1-weighted transverse spin-echo images (TR = 1000 ms, TE = 12 ms, 118 μm × 118 μm × 1 mm resolution) were rather indistinguishable (right). T_2-weighted images of kidneys (left) in cisplatin-treated (middle), cisplatin + BGP-15-treated (lower) and untreated (upper) mice are shown. Kidney of cisplatin-treated mice showed marked increase of intensity in the peripheral regions (arrow). In animals treated with cisplatin and BGP-15 the increase in intensity was considerably smaller. For imaging parameters see Section 2.

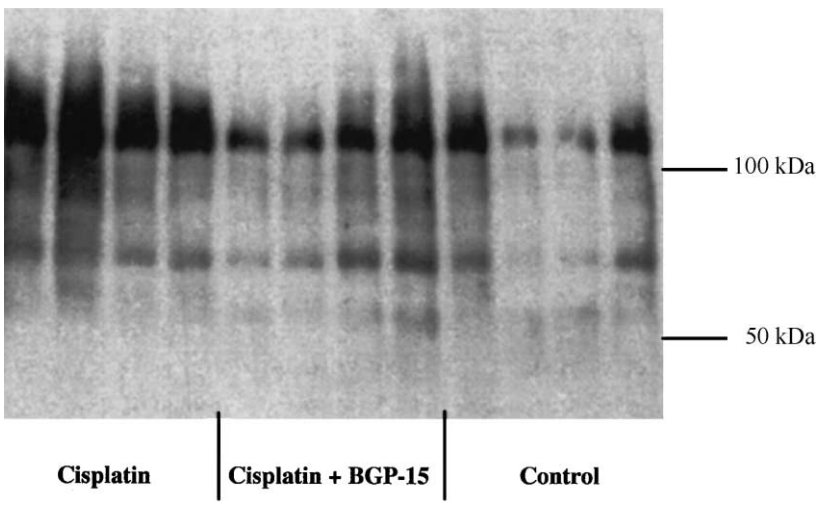

Fig. 6. Analysis of poly-ADP-ribosylation in the kidney. Equal amount of kidney proteins were separated on SDS-PAGE gel and were transferred to Hybond-P membrane. Poly-ADP-ribosylation was detected by anti-poly(ADP-ribose) polyclonal antibody (LP96-10) and it was visualized with enhanced chemiluminescence reagent.

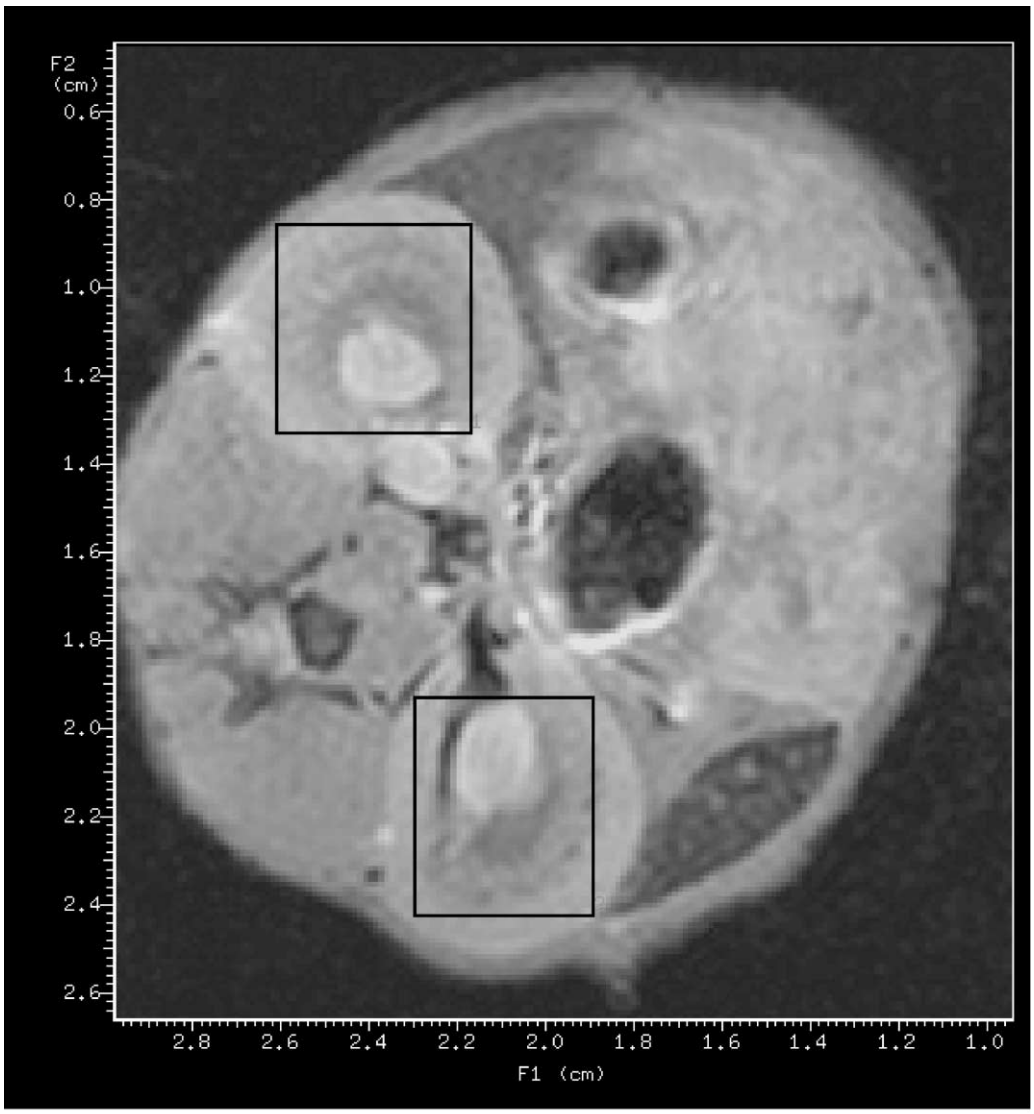

(a)

Fig. 7. (a) The voxels of interest for two subsequent localized experiments are marked with rectangles in a typical spin-echo scout image (TR = 1000 ms, TE = 12 ms) representing a transversal slice of a mouse abdomen. (b) Representative spectra of localized NMR spectroscopy. The observed peaks represent the following species: P_i (ca. 5 ppm), creatine phosphate (0.0 ppm), γ-ATP + β-ADP (−2.5 ppm), α-ATP + α-ADP + NAD^+ + NADH (−7.5 ppm), β-ATP (−16 ppm). (1) Control, (2) cisplatin, (3) cisplatin + BGP-15.

status of kidney during cisplatin-induced nephrotoxicity. It elevated the decreased glutathione and catalase levels, but did not affect SOD activity. BGP-15 treatment decreased the cisplatin-caused ROS production and restored the level of high energy phosphate intermediates. While BGP-15 protected against cisplatin-induced nephrotoxicity, it did not reduce the antitumor efficacy of this cytostatic agent. Tumor growth inhibition by cisplatin was identical in the presence and absence of BGP-15 in several cancer cell lines and in two transplantable solid mouse tumors (S-180, B-16). In addition, BGP-15 increased the survival of cisplatin-treated P-388 leukemia bearing mice.

Reduced renal blood flow and proximal tubular injury are considered as primary tissue alterations in the pathogenesis of cisplatin-induced nephrotoxicity. The exact subcellular and molecular targets and the precise mechanism of damage are being debated. A series of relevant observations indicate that generation of free oxygen radicals in tubular cells plays a crucial role in the pathogenic process [6,20]. Increased level of oxygen radicals (superoxide anion and hydroxyl radicals) was observed after cisplatin treatment [3]. It has been suggested that cisplatin induced release of free iron may have a role in the generation of ROS [21]. Free radical scavengers and antioxidants, such as SOD [22], α-tocopherol, ascorbic acid, ebselen, and glutathione protect against cisplatin-induced nephrotoxicity, whereas buthionine sulfoximide, a GSH depleting compound potentiates that [23]. Depletion of GSH below a critical level seems to trigger lipid peroxidation and further alterations in mitochondria [24].

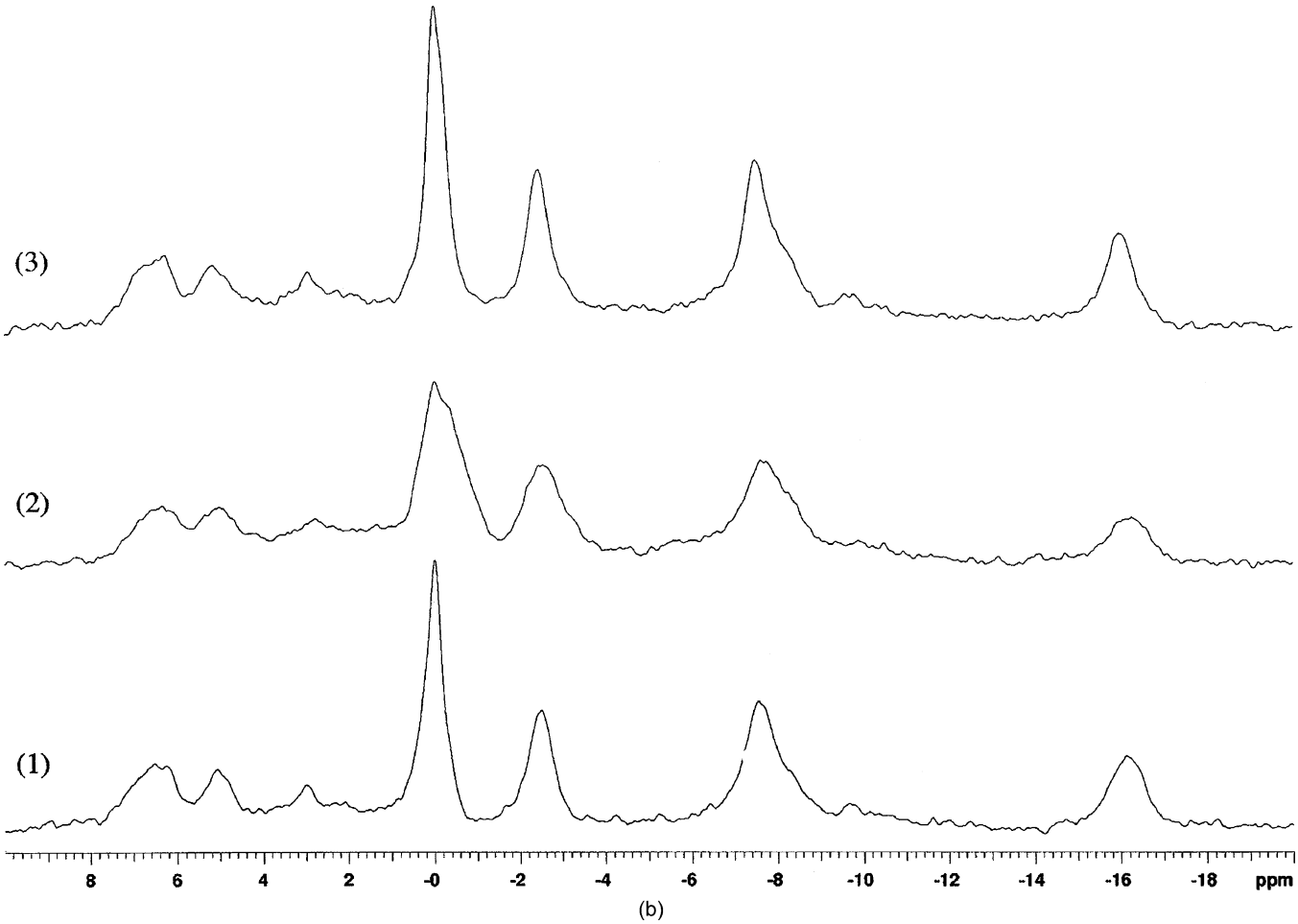

Fig. 7. (*Continued*).

Decreased SOD, catalase, glutathione-peroxidase activities have been observed after cisplatin treatment, which diminishes the ability of the kidney to neutralize H_2O_2 and lipid peroxides [7]. Anticancer or anti-viral drugs can cause DNA damage both directly and indirectly through the elevated level of ROS [9,18]. DNA damage triggers a series of adaptive and repair mechanisms including the activation of PARP. PARP has a dual role in response to

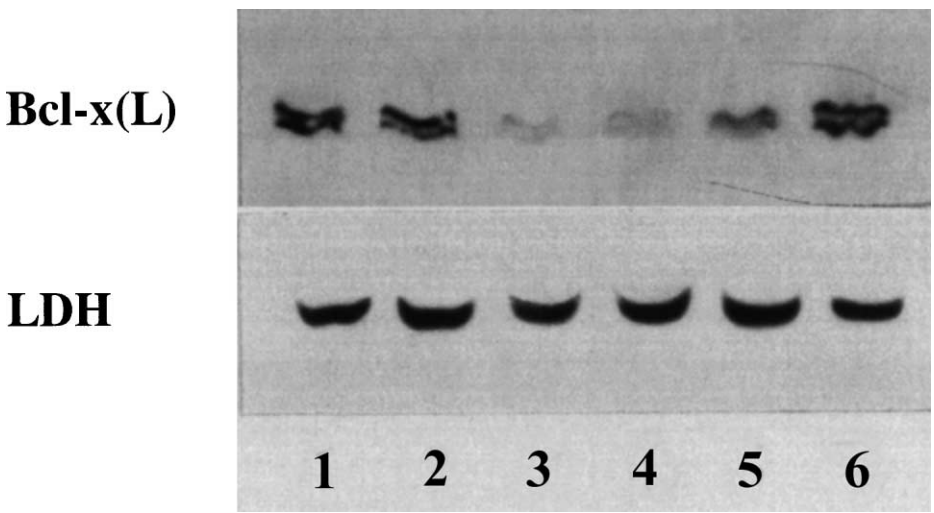

Fig. 8. Effect of cisplatin and BGP-15 treatment on the Bcl-x content of mice kidney mitochondria. Lanes: 1, 2 control; 3, 4 cisplatin-treated; 5, 6 cisplatin + BGP-15-treated. The lanes were loaded with equal amount of protein. Control protein: LDH.

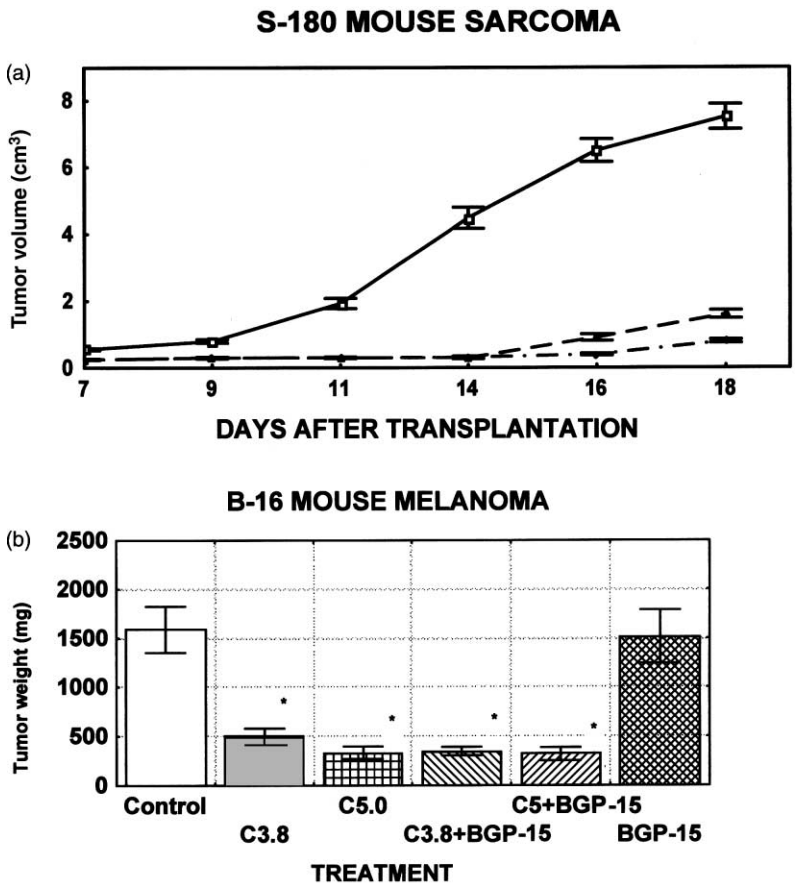

Fig. 9. Effect of BGP-15 on the antitumor activity of cisplatin in S-180 mouse sarcoma (a) and B-16 mouse melanoma (b). Tumor cells were transplanted subcutaneously. Tumor size was measured with a caliper (S-180) or the weight of the excised tumor was determined 7 days after the cisplatin treatment (B-16). Treatment: (a) (□) control, (▲) cisplatin 10 mg/kg, i.p., (◆) cisplatin 10 mg/kg i.p. + BGP-15 200 mg/kg, p.o., (b) C3.8, C5 = 5 × 3.8 mg/kg and 5 × 5 mg/kg cisplatin i.p., C3.8 + BGP-15, C5 + BGP-15 = 5 × 3.8 mg/kg, or 5 × 5 mg/kg cisplatin + 200 mg/kg BGP-15 p.o. daily. Data represent mean ± SEM. The asterisk (∗) values are different ($P < 0.05$) relative to control (ANOVA Post-hoc Duncan).

DNA damage. It recognizes DNA breaks and binds to histones at the damaged site. Poly-ADP-ribosylation of histones destabilizes the chromatin structure and makes it accessible to DNA repair enzymes thereby initiating the assembly of the DNA repair complex [25]. Whereas PARP participates in averting cell damage, its excessive activation can have deleterious effect, as well. This is due to an abnormally increased consumption of NAD^+ that PARP uses for building up poly(ADP-ribose) chains. This activity leads to depletion of cellular NAD^+, and subsequently ATP

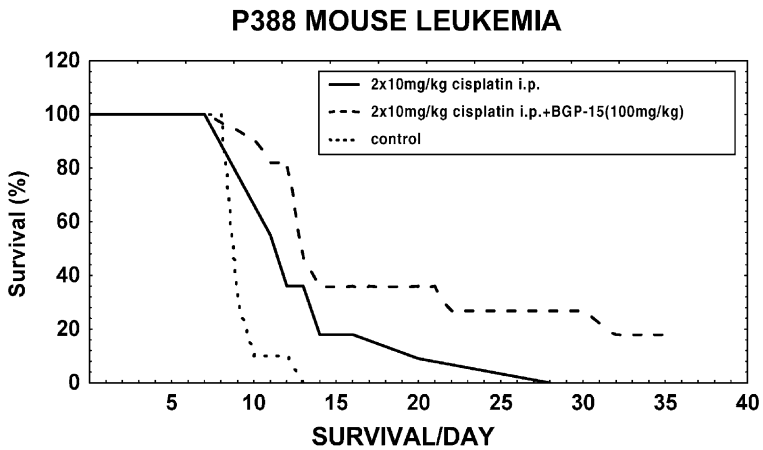

Fig. 10. Effect of BGP-15 on the antitumor efficacy of cisplatin in P-388 mouse leukemia. Mice were injected with 5×10^6 leukemia cells i.p. Cisplatin treatment started on the third day. The difference in survival time between cisplatin- and cisplatin + BGP-15-treated groups was compared with Wilcoxon test ($P = 0.02683$).

resulting in metabolic collapse and eventually in cell death [26–28].

It has been demonstrated that PARP inhibition is beneficial in various conditions with oxidative injury (hypoxia-reoxygenation, streptozotocin-induced diabetes, and inflammation) [10,29,30]. The PARP inhibitor and tissue protective effect of BGP-15 against oxidative damage has been demonstrated in several *in vitro* and *in vivo* systems [10]. In this study, we have shown that BGP-15 inhibits the cisplatin-induced poly-ADP-ribosylation in the kidney. At the same time, BGP-15 restored the cisplatin-induced disturbance in energy metabolism and preserved the ATP level in the protected tissue. This activity may well be the most important mechanism of this protection. In addition, BGP-15 can directly protect the mitochondria [10]. Considering the role of oxidative damage in the nephrotoxic effect of cisplatin, it is not surprising that PARP inhibitors can alleviate these side effects. To our best knowledge, the present work provides the first experimental evidence for it. Furthermore, the protection of renal GSH content indicates that PARP inhibition has beneficial influence on the antioxidant status in cisplatin-induced oxidative stress. The observed modest inhibition of cisplatin induced increase in ROS production by mitochondria and the prevention of the loss of Bcl-x are in accordance with the proposed mechanism of BGP-15. The increased catalase activity may contribute to the nephroprotective effect, but further study is needed to determine whether this change is a cause or rather consequence of the nephroprotective effect.

A very important observation is that BGP-15 does not diminish the antitumor activity of cisplatin in several *in vitro* and *in vivo* systems. Furthermore, co-administration of BGP-15 increased the survival of cisplatin-treated P-388 leukemia bearing mice. A possible explanation for this observation is that cisplatin affects DNA both directly and indirectly. The antitumor activity of cisplatin depends on its direct interaction with the DNA. The cisplatin–DNA adducts are repaired primarily by nucleotide excision repair, a process which is PARP independent [31]. Cisplatin, however, also inflicts a less specific damage to the genetic material via ROS generation. The cisplatin-induced oxidative damage should affect tumor tissues less seriously for several reasons. Tumors usually grow in hypoxic environment, they contain a greatly reduced number of mitochondria and rely mostly on glycolysis for energy. These conditions do not favor the generation of free radicals. The cisplatin-induced, ROS-mediated damages affect predominantly well-oxygenated normal tissues like the kidney, where the cisplatin concentration is especially high. Inhibition of PARP prevents an excessive activation of the enzyme in normal cells which would otherwise cause an energy crisis and subsequently cell death.

The presented data suggest that BGP-15 is a potentially effective chemoprotective agent, which can prevent nephrotoxicity of cisplatin without compromising its antitumor activity. BGP-15, which is not a sulfhydryl group-based scavenger, represents a new type of chemoprotective compounds. The chemoprotective activity of BGP-15 seems to rely on the modulation of PARP activity. Furthermore, considering the mitochondrion-protective effect of PARP inhibitors [10,26], and the protective activity of BGP-15 against the AZT-induced mitochondrial damage [32], the chemoprotective activity of BGP-15 presumably involves direct protection of mitochondria as well. Efficacy of BGP-15 is comparable to that of amifostine, the most frequently used chemoprotective agent. It is, however, a clear advantage that BGP-15 is active orally, whereas amifostine should be administered intravenously. Our most recent data indicate that the chemoprotective activity of BGP-15 is not limited to cisplatin but exists in combination with other antitumor agents, as well.

Acknowledgments

We are grateful to Michael J. Brownstein and Wayne Bardin for helpful comments on the manuscript.

References

[1] Tognella S. Pharmacological interventions to reduce platinum-induced toxicity. Cancer Treat Rev 1990;17:139–42.
[2] Spencer CM, Goa KL. Amifostine: a review of its pharmacodynamic and pharmacokinetic properties, and therapeutic potential as a radio-protector and cytotoxic chemoprotector. Drugs 1995;50(6):1001–31.
[3] Matsuda H, Tanaka T, Takaham AU. Cisplatin generates superoxide anion by interaction with DNA in a cell free system. Biochem Biophys Res Commun 1994;203:1175–80.
[4] Kruidering M, van de Water B, de Heer E, Mulder GJ, Nagelkerke JF. Cisplatin-induced nephrotoxicity in porcine proximal tubular cells: mitochondrial dysfunction by inhibition of complexes I to IV of respiratory chain. J Pharmacol Exp Ther 1997;280:638–49.
[5] Hannemann J, Baumann K. Cisplatin-induced lipid peroxidation and decrease of gluconeogenesis in rat kidney cortex: different effects of antioxidants and radical scavengers. Toxicology 1988;51:119–32.
[6] Matsushima H, Yonemura K, Ohishi K, Hishida A. The role of oxygen free radicals in cisplatin-induced acute renal failure in rats. J Lab Clin Invest 1998;131:518–26.
[7] Husain K, Morris C, Whiteworth C, Trammel GL, Rybak LP, Momani SM. Protection by ebselen against cisplatin-induced nephrotoxicity. Antioxidant Syst Mol Cell Biochem 1998;178:127–33.
[8] Zhang J, Lindup E. Role of mitochondria in cisplatin-induced oxidative damage exhibited by rat renal cortical slices. Biochem Pharmacol 1993;45:2215–22.
[9] Burkle A, Chen G, Kupper JH, Grube K, Zeller WJ. Increased poly(ADP-ribosyl)ation in intact cells by cisplatin treatment. Carcinogenesis 1993;14:559–61.
[10] Szabados E, Literati-Nagy P, Farkas B, Sumegi B. BGP-15, a nicotinic amidoxime derivative protecting heart from ischemia reperfusion injury through modulation of poly(ADP-ribose) polymerase. Biochem Pharmacol 2000;59:937–45.
[11] Fawcett JK, Scott JE. A rapid precise method for the determination of urea. J Clin Pathol 1960;13:156–7.

[12] Chaney AL, Marbach P. Modified reagents for determination of urea and ammonia. Clin Chem 1962;8:130–3.
[13] Henry JB. Clinical diagnosis and management. 17th ed. London: Saunders, 1984.
[14] Larsen K. Creatinine assay by a reactionkinetic principle. Clin Chim Acta 1972;66:209.
[15] Beutler F, Duron O, Kelly BM. Improved method for the determination of blood glutathione. J Lab Clin Med 1963;61: 882–8.
[16] Aebi H. Catalase *in vitro*. Meth Enzymol 1984;105:121–6.
[17] Misra HP, Fridovich I. The role of superoxide anion in the autooxidation of epinephrine and a simple assay for superoxide-dismutase. J Biol Chem 1972;247:3170–5.
[18] Szabados E, Fischer GM, Toth K, Csete B, Nemeti B, Trombitas K, Habon T, Endrei D, Sumegi B. Role of reactive oxygen species and poly(ADP-ribose) polymerase in the development of AZT-induced cardiomyopathy in rat. Free Radic Biol Med 1999;26:309–17.
[19] Monks A, Scudiero D, Skehan P, Shoemaker R, Paull K, Vistica D, Hose C, Langley J, Cronise P, Vaigro-Wolff A. Feasibility of a high-flux anticancer drug screen using a diverse panel of cultured human tumor cell lines. J Natl Cancer Inst 1991;83:757–66.
[20] Sugihara K, Gemba M. Modification of cisplatin toxicity by antioxidants. Jpn J Pharmocol 1986;40:353–5.
[21] Balig R, Zhanf Z, Baliga M, Ueda N, Shah S. *In vitro* and *in vivo* evidence suggesting a role for iron in cisplatin-induced nephrotoxicity. Kidney Int 1998;53:394–401.
[22] McGinness FE, Proctor PH, Demopoulos HB, Hokanson JA, Kirkpatrick DS. Amelioration of cisplatin nephrotoxicity by orgotein (superoxide dismutase). Physiol Chem Phys 1978;10:267–77.
[23] Sugihara K, Nakano S, Koda M, Tanaka N, Gemba M. Stimulatory effect of cisplatin on production of lipid peroxidation in renal tissues. Jpn J Pharmacol 1987;43:247–52.
[24] Kameyama Y, Gemba M. Cisplatin-induced injury to calcium uptake by mitochondria in glutathione-depleted slices of rat kidney cortex. Jpn J Pharmacol 1993;55:174–6.
[25] Lindahl T, Satoh MS, Poirier GG, Klungland A. Post-translational modification of poly(ADP-ribose) polymerase induced by DNA strand breaks. Trends Biochem Sci 1995;20:405–11.
[26] Virag L, Salzman AL, Szabo C. Poly(ADP-ribose) synthetase activation mediates mitochondrial injury during oxidant-induced cell death. J Immunol 1998;161:3753–9.
[27] Cuzzocrea S, Zingarelli B, Caputi AP. Peroxynitrate-mediated DNA strand breakage activates poly(ADP-ribose) synthetase and causes cellular energy depletion in a nonseptic shock model induced by zymosan in the rat. Shock 1998;9:336–40.
[28] Szabo C, Zingarelli B, O'Connor M, Salzman AL. DNA strand breakage, activation of poly(ADP-ribose) synthetase, and cellular energy depletion are involved in the cytotoxicity of macrophages and smooth muscle cells exposed to peroxynitrite. Proc Natl Acad Sci USA 1996;93:1753–8.
[29] Szabó C, Dawson VL. Role of poly(ADP-ribose) synthetase in inflammation and ischemia-reperfusion. TIBS 1998;19:287–98.
[30] Zingarelli B, Cuzzocrea S, Zsengeller Z, Salzman AL, Szabo C. Protection against myocardial ischemia and reperfusion injury by 3-aminobenzamide, an inhibitor of poly(ADP-ribose) synthetase. Cardiovasc Res 1997;36:205–15.
[31] Simbulan-Rosenthal CM, Rosenthal DS, Ding R, Bhatia K, Smulson ME. Prolongation of the p53 response to DNA strand breaks in cells depleted of PARP by antisense RNA expression. Biochem Biophys Res Commun 1998;253(3):864–8.
[32] Sumegi B, Rabloczky G, Rácz I, Tory K, Bernath S, Varbiro G, Gallyas Jr F, Literati-Nagy P. Protective effect of PARP inhibitors against cell damage induced by antiviral and anticancer drugs. In: Szabo C, editor. Cell death: the role of poly(ADP-ribose)polymerase, Pharmacology and Toxicology Series. Boca Raton: CRC Press, 2000. p. 167–82.